Ideal tensile strength and band gap of single-walled carbon nanotubes

Shigenobu Ogata and Yoji Shibutani
Department of Mechanical Engineering and Systems, Handai Frontier Research Center, Osaka University, Osaka 565-0871, Japan
(Received 3 July 2003; published 20 October 2003)

The ideal tensile (compressive) strength, Young's modulus, and band-gap changes of single-walled carbon nanotubes (SWNT's) with zigzag types of (8,0), (9,0), and (10,0) and armchair of (8,8) under an uniaxial deformation are analyzed using a tight binding (TB) method parametrized by Tang *et al.* In addition, the first principle density functional theory based on the local density approximation (DFT) is employed as a cross-check. It is well known that the band gap of a SWNT changes according to the uniaxial strain. Most of the previous studies have represented the deformed atomic structure by an empirical potential and then applied band analysis to estimate the band gaps. However, this step-by-step process may allow errors due to the lack of transferability of the empirical potentials in the highly deformed state. In this study, in order to estimate the electronic structure change more accurately and examine the transferability of the TB potential, we used the TB and also the DFT method to find equilibrium atomic structures of the SWNT's deformed by applied strain. At the same time, the band gaps of the equilibrium structure are estimated. We find that the TB results for ideal strengths, Young's modulus, and band gaps are basically in good agreement with the DFT results. The band-gap changes are in qualitative agreement with Yang's theory in which a uniform deformation is assumed. However, even though the theory predicts a zero gap for the armchair SWNT's, we see a finite band gap of the (8,8) SWNT at the 20% tensile strain level, which is the extreme strain sustained immediately succeeding failure.

DOI: 10.1103/PhysRevB.68.165409 PACS number(s): 61.48.+c, 62.20.Dc, 62.20.Fe, 71.20.Tx

Single-walled carbon nanotubes (SWNT's) discovered by Iijima[1] are known to possess attractive practical mechanical and electronic characteristics. The extremely high Young's modulus has been experimentally confirmed[2–4] as predicted by theoretical studies.[5–9] It clearly surpasses that of commercial carbon fiber. At the same time, their one-dimensional electronic structure leads to a change of band gap with a change in a geometric property.[10–15] This opens up the possibility of a nanoscale switching mechanism in SWNT's.

It seems evident, therefore, that the electronic states of SWNT's could be coupled with their finite mechanical deformation behavior. However, there are few studies that have examined this complex coupled behavior. In the present report, we calculate the atomistic and electronic structure changes under tensile (compressive) deformation by a tight binding (TB) calculation. As a cross-check, we relate these calculations to a first principles density functional theory based on the local density approximation (DFT). We then discuss the ideal tensile strength of the SWNT's and their band gaps.

We selected the following SWNT's: zigzag type (8,0), (9,0), and (10,0), and armchair type (8,8). The axial direction (z) of these SWNT's was selected as the tensile direction. By applying tensile strain in the TB and DFT simulations, we evaluated the relaxed ideal tensile strengths, which can be defined as the maximum axial tensile strength of SWNT's of σ_{zz}^{Y}.

Simultaneously, the band-gap changes during the tensile tests were assessed. The axial stress σ_{zz} was estimated by calculating the axial force acting on the SWNT divided by the cross sectional area of the initial atomic configuration of the SWNT. To calculate this cross sectional area we considered the interlayer distance of graphite (3.35 Å) to be the thickness of the SWNT. For the initial atomic configuration, we chose an ideal atomic configuration, which can be uniquely determined by the two coefficients, n_1 and n_2, of the chiral vector (n_1,n_2) and the experimentally determined C-C bond length in graphite ($d=1.42$ Å). Therefore the z dimension of a simulation supercell, which includes the primitive unit structure of the SWNT, was also uniquely determined. The strain meshes in z, $\Delta\varepsilon_{zz}$, of the numerical tensile tests were selected as 0.4% and 1.0% for the TB and the DFT calculations, respectively. The dimensions of the x and y directions were kept constant during the tensile test. By using a simulated annealing method in the TB and a conjugate gradient method in the DFT, the force on each atom in each strain level was relaxed to less than 0.01 eV/Å. The dimensions of the simulation supercells employed in these calculations are tabulated in Table I. To avoid an effect of the periodic boundary condition, the cell dimensions in the x and y directions should be set sufficiently large. By using the tabulated cell dimensions, the maximum stresses in the x and y directions, <2GPa during all the tests, can be kept much smaller than the axial stresses.

TABLE I. Supercell dimensions (x,y,z) in nm used in the TB and DFT calculations.

	(8,0)	(9,0)	(10,0)	(8,8)
TB	(3.13, 3.13, 0.426)	(3.91, 3.91, 0.426)	(3.52, 3.52, 0.426)	(5.42, 5.42, 0.246)
FP	(1.25, 1.25, 0.426)	(1.57, 1.57, 0.425)	(1.41, 1.41, 0.425)	(2.17, 2.17, 0.245)

 ©2003 The American Physical Society

TABLE II. Axial strains ε_{zz}^{0} of the relaxed structures measured from the ideal structures.

	(8,0)	(9,0)	(10,0)	(8,8)
TB	−0.0058	−0.0052	−0.0020	−0.0009
FP	−0.0110	−0.0099	−0.0097	−0.0066

The parameter set proposed by Tang *et al.*[16] was used for the TB calculations. It has already been confirmed that this parameter set produces accurate volume energy curves of the fcc, bcc, sc, graphite, diamond, and one-dimensional chain structure of carbon[17] by comparing its results with curves produced by the DFT. For the DFT calculations performed in the present study, the Vienna *ab initio* simulation package[18] (VASP) was used throughout with the Cepley-Alder local density approximation (LDA) functional[19] as parametrized by Perdew and Zunger.[20] The ultrasoft (US) pseudopotential[21] supplied in VASP was used. The plane-wave energy cutoff was taken to be $E_{\mathrm{cut}}=286.6$ eV. It has been shown that the ideal strength calculation obtained through this method is reliable.[22] Brillouin zone (BZ) **k**-point sampling was done using the Monkhorst-Pack algorithm,[23] and $1\times1\times4$ **k**-points were chosen for both the TB and the DFT calculations. **k**-point convergence has been carefully checked for all the supercells.

Before we started the tensile test, the z dimension of the supercells and the initial atomic configuration were completely relaxed in both the TB and DFT calculations. Then, the axial strains of the relaxed equilibrium atomic structures, ε_{zz}^{0}, measured from the initial atomic configuration were evaluated. These are listed in Table II. By both methods, contractions less than 1% can be seen in all SWNT's. The zigzag SWNT's show a higher contraction in z than does the armchair SWNT. These relaxed z dimensions of the supercells were used as a reference when calculating the applied strains in the following discussion.

The band-gap versus strain curves and the stress versus strain curves determined for each SWNT during the tensile tests are shown in Figs. 1(a)–1(d) and Figs. 2(a)–2(d), respectively. We estimate the Young's moduli of the SWNT's from the slope of the stress-strain curves at $\varepsilon_{zz}=0$. These are listed in Table III. The TB results agree well with the DFT results, and the DFT results are in excellent agreement with recent theoretical studies.[5–9] They fit within the range of the recent experimental results, 300–1900 GPa (Refs. 2–4); the average is ~1000 GPa.

It should be recalled that the values in Table III were all calculated using the graphite interlayer distance $h=3.35$ Å as the thickness of the SWNT. The Young's moduli are very close to the in-basal plane Young's modulus of graphite at 0 K of $E_{\mathrm{gs}}=1090$ GPa,[25] and do not strongly depend on the diameter and type of the SWNT's that have a diameter larger than 6 Å . This fact has been clearly shown by Chang and Gao.[9] The band gap changes found by TB and DFT during the tensile tests are very similar [Figs. 1(a)– 1(d)]; in almost the entire strain region, these results can be predicted by an analytical formulation using the Hückel TB model[13] in which a uniform tensile deformation is assumed. However, in spite

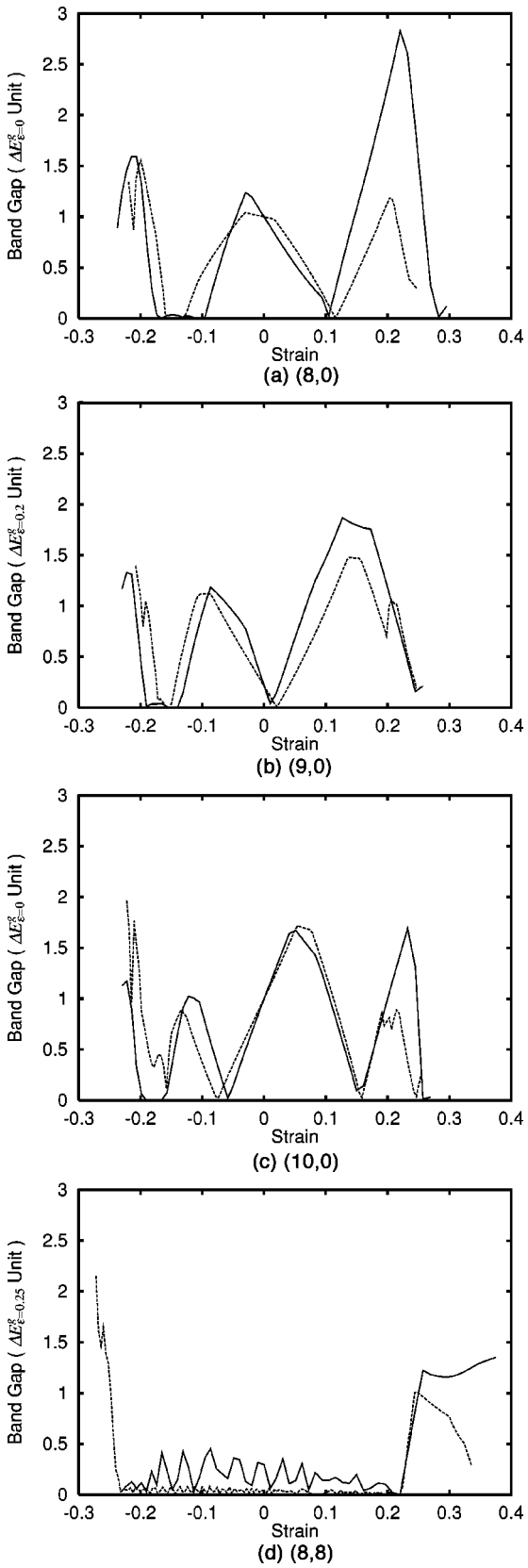

FIG. 1. Band gap (ΔE^{g}) versus strain (ε_{zz}) curves of (a) (8,0), (b) (9,0), (c) (10,0), and (d) (8,8) SWNT's. Dashed lines and solid lines represent the TB and FP results, respectively. The band gap is normalized by the value at a strain level, $\varepsilon=0$ for the (8,0) and (10,0), $\varepsilon=0.2$ for the (9,0), and $\varepsilon=0.25$ for the (8,8).

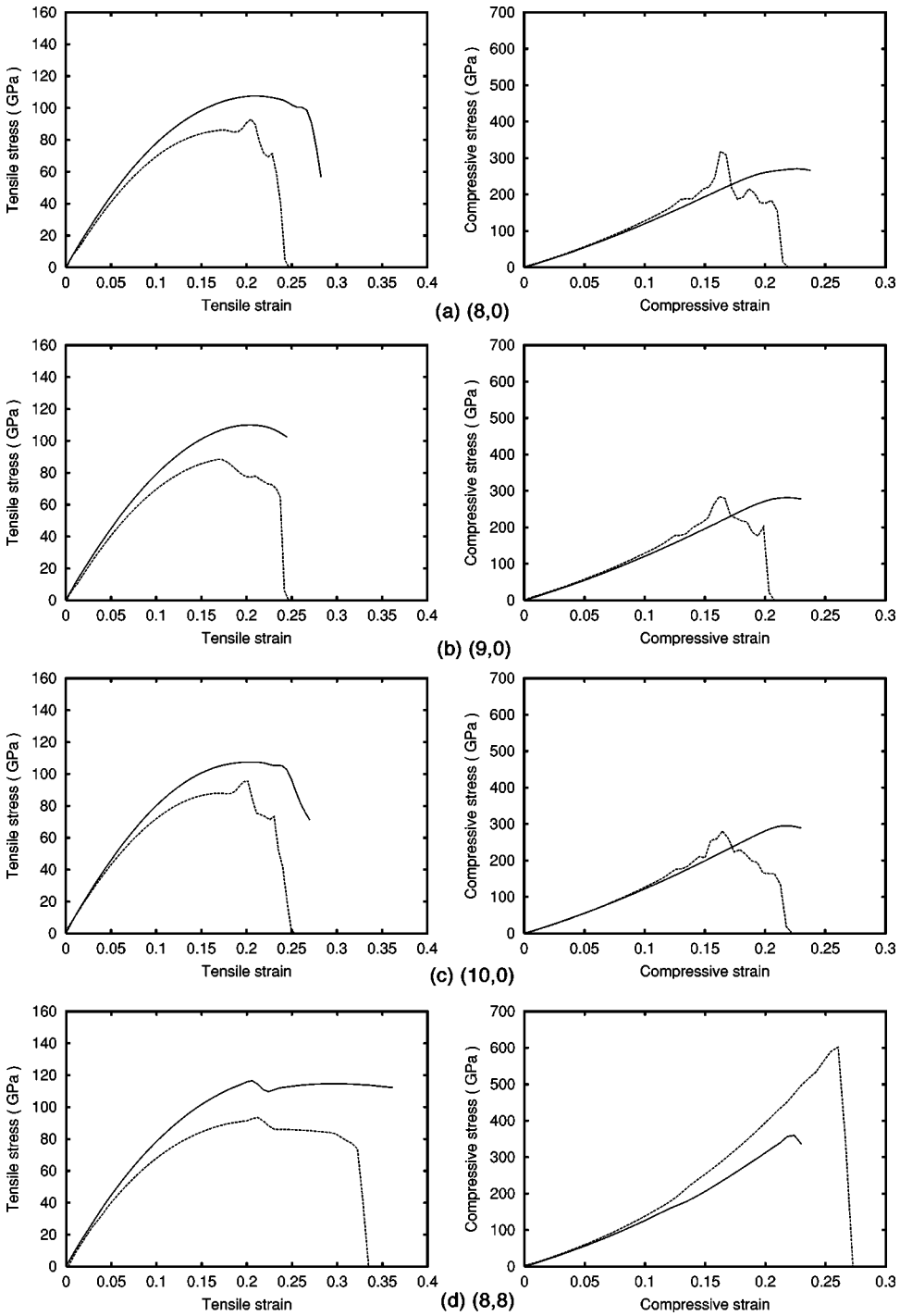

FIG. 2. Tensile and compressive stress (σ_{zz}) along the axial direction versus strain (ε_{zz}) curves of (a) (8,0), (b) (9,0), (c) (10,0), and (d) (8,8) SWNT's. Dashed lines and solid lines represent the TB and FP results, respectively.

of the fact that this formulation predicts a zero gap for the (8,8) SWNT, we see a clear hump at a 20% tensile strain in both the TB and DFT results. At this strain level, the stress starts to decrease [Fig. 2(d)]; that is, the structure has already become unstable. We find a local geometric instability which induces a small discontinuity in a bond angle and length changes. However, the (8,8) SWNT still retains a tube structure without any failure under conditions of controlled strain. If instead we control the tensile load, we never observe the unstable state. It is worth noting that band gaps calculated by both the DFT and TB may not have good quality in terms of quantitative determination. However, usually they give good qualitative estimations. Therefore, in Fig. 1 we normalized the band-gap data by the data of a strain.

TABLE III. Estimated Young's moduli of the SWNT's (in GPa).

	(8,0)	(9,0)	(10,0)	(8,8)
TB	969	974	965	979
FP	1002	1017	972	1008

For the stress-strain curves [Figs. 2(a)–2(d)], the TB method basically gives smaller values in the tensile (not the

TABLE IV. Ideal tensile strengths (σ_{zz}^{Y}, in GPa) and strains (ε_{zz}^{crit}) of SWNT's calculated by the TB and FP methods. C and T denote compressive and tensile, respectively. E is Young's modulus of the SWNT.

	(8,0)			(9,0)			(10,0)			(8,8)		
	σ_{zz}^{Y}	σ_{zz}^{Y}/E	ε_{zz}^{crit}	σ_{zz}^{Y}	σ_{zz}^{Y}/E	ε_{zz}^{crit}	σ_{zz}^{Y}	σ_{zz}^{Y}/E	ε_{zz}^{crit}	σ_{zz}^{Y}	σ_{zz}^{Y}/E	ε_{zz}^{crit}
TB (C)	−321.1	−0.331	−0.163	−288.2	−0.296	−0.164	−287.3	−0.298	−0.166	−624.0	−0.637	−0.265
FP (C)	−270.2	−0.270	−0.230	−281.0	−0.276	−0.222	−295.1	−0.304	−0.214	−362.2	−0.359	−0.222
TB (T)	86.8	0.090	0.211	88.4	0.091	0.170	95.6	0.099	0.198	93.0	0.095	0.207
FP (T)	107.5	0.110	0.208	109.9	0.108	0.208	107.4	0.110	0.208	114.6	0.114	0.295

compressive) stress than the DFT method. However, the TB results are in reasonable agreement with the DFT results in both the tensile and the compressive tests. We listed the maximum values of tensile and compressive stresses in Table IV with corresponding critical strains ε_{zz}^{crit}. These values can be defined as the ideal tensile strength (ITST-T, σ_{zz}^{YT}) and compressive strength (ITST-C, σ_{zz}^{YC}). The σ_{zz}^{YC} decreases in the order of (8,0), (9,0), (10,0), and (8,8) in the DFT calculations and the σ_{zz}^{YT} does not depend on the type of the SWNT's. The ITST-T and Young's modulus ratio, σ_{zz}^{YT}/E, are almost equal in the tensile tests and σ_{zz}^{YC}/E decreases in the order of (8,0), (9,0), (10,0), and (8,8) in the compressive tests. Therefore, the Young's modulus is a useful predictor of σ_{zz}^{YT} in tensile tests, but not of σ_{zz}^{YC} in compressive tests.

We must note that we observe only the local buckling in these compressive simulations. The Euler-type buckling[26] observed in the macroscopic tube under compression cannot be seen because of the small supercell dimension in z. More generally, since the value of the ITST-C depends on the length of the tube structure, we have to take into account the tube length for its estimation. However, the ITST-C may reasonably be defined as a maximum compressive stress of the unit structure of a SWNT, as calculated in our study. This maximum is definitely an upper bound of the compressive stress on the SWNT. The zigzag (8,0), (9,0), and (10,0) SWNT's show a sharp drop in stress beyond the critical strain in tension. In contrast, we see very ductile behavior in the (8,8) case, as also found by Umeno *et al.*[24] using the same TB calculation as us. Hence, we find that the zigzag SWNT's change their properties from metallic to semiconductor or from semiconductor to metallic within the range of stable deformation, and that the armchair SWNT exhibits a transition to semiconductor from metallic before its failure.

We thank Ayumi Ogawa very much for the TB calculations and acknowledge the financial support of the Handai Frontier Research Center.

[1] S. Iijima, Nature (London) **354**, 56 (1991).
[2] A. Krishnan, E. Dujardin, T. W. Ebbesen, P. N. Yianilos, and M. M. J. Treacy, Phys. Rev. B **58**, 14 013 (1998).
[3] S. Akita, H. Nishijima, T. Kishida, and Y. Nakayama, Jpn. J. Appl. Phys., Part 1 **39**, 3724 (2000).
[4] M. F. Yu, B. S. Files, S. Arepalli, and R. S. Ruoff, Phys. Rev. Lett. **84**, 5552 (2000).
[5] D. Sanchez-Portal, E. Artacho, J. M. Soler, A. Rubio, and P. Ordejon, Phys. Rev. B **59**, 12 678 (1999).
[6] Z. Xin, Z. Jianjun, and O. Y. Zhong-can, Phys. Rev. B **62**, 13 692 (2000).
[7] C. Q. Ru, Phys. Rev. B **62**, 10 405 (2000).
[8] Z. C. Tu and O. Y. Zhong-can, Phys. Rev. B **65**, 233407 (2002).
[9] T. Chang and H. Gao, J. Mech. Phys. Solids **51**, 1059 (2003).
[10] R. Saito, M. Fujita, G. Dresselhaus, and M.S. Dresselhaus, Appl. Phys. Lett. **60**, 2204 (1992).
[11] A. Rochefort, P. Avouris, F. Lesage, and D.R. Salahub, Phys. Rev. B **60**, 13 824 (1999).
[12] C. Kilic, S. Ciraci, O. Gulseren, and T. Yildirim, Phys. Rev. B **62**, R16 345 (2000).
[13] L. Yang and J. Han, Phys. Rev. Lett. **85**, 154 (1999).
[14] M. Ouyang, J. Huang, C.L. Cheung, and C.M. Lieber, Science **292**, 702 (2001).
[15] J.W. Ding, X.H. Yan, and J.X. Cao, Phys. Rev. B **66**, 073401 (2002).
[16] M. S. Tang, C. Z. Wang, C. T. Chan, and K. M. Ho, Phys. Rev. B **53**, 979 (1996).
[17] T. Kugimiya, Ph.D. thesis, Osaka University (2001).
[18] VASP: G. Kresse and J. Hafner, Phys. Rev. B **47**, 558 (1993); G. Kresse and J. Furthmüller, *ibid.* **54**, 11 169 (1996).
[19] D. M. Ceperley and B. J. Alder, Phys. Rev. Lett. **45**, 566 (1980).
[20] J. P. Perdew and A. Zunger, Phys. Rev. B **23**, 5048 (1981).
[21] D. Vanderbilt, Phys. Rev. B **41**, 7892 (1990).
[22] S. Ogata, J. Li, and S. Yip, Science **298**, 807 (2002).
[23] H.J. Monkhorst and J.D. Pack, Phys. Rev. B **13**, 5188 (1976).
[24] Y. Umeno, T. Kitamura, and E. Matsui, J. Soc. Mat. Sci. Jpn. **52**, 219 (2003).
[25] Landolt-Bornstein III/29a (Springer, Heidelberg, 1992).
[26] J. M. Gere and S. P. Timoshenko, *Mechanics of Materials* (PWS, Boston, 1990).